Pacific Graphics (2019)
C. Theobalt, J. Lee, and G. Wetzstein (Editors)

Short Paper

A Psychophysical Analysis of Fabricated Anisotropic Appearance

J. Filip, M. Kolafová, R. Vávra

The Czech Academy of Sciences, Institute of Information Theory and Automation, Prague, Czech Republic

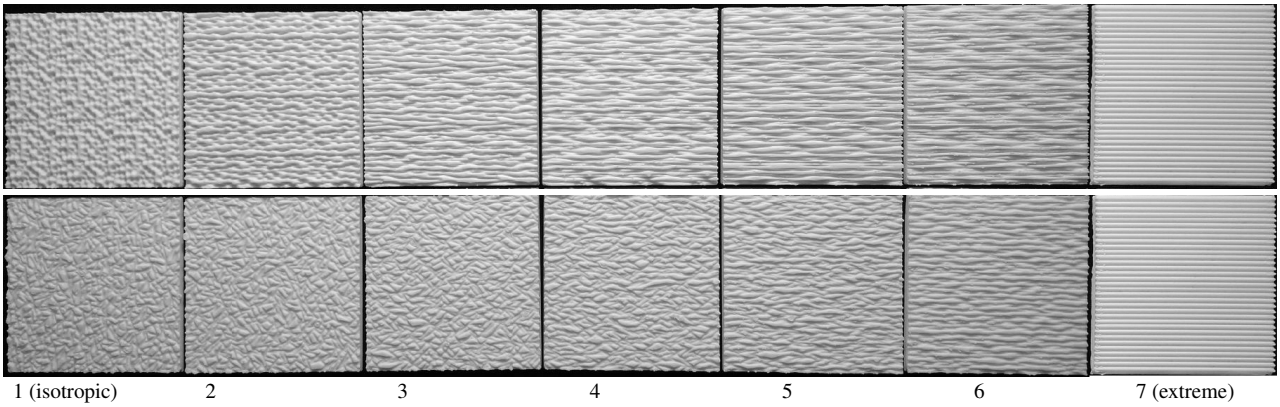

Figure 1: *3D printed anisotropic effects A (the top row) and B (the bottom row) illuminated from the top.*

Abstract

Many materials change surface appearance when observed for fixed viewing and lighting directions while rotating around its normal. Such distinct anisotropic behavior manifests itself as changes in textural color and intensity. These effects are due to structural elements introducing azimuthally-dependent behavior. However, each material and finishing technique has its unique anisotropic properties which are often difficult to control. To avoid this problem, we study controlled anisotropic appearance introduced by means of 3D printing. Our work tends to link perception of directionality with perception of anisotropic reflectance effect it causes. We simulate two types of structure-based anisotropic effects, which are related to directional principles found in real-world materials. For each type, we create a set of test surfaces by controlling the printed anisotropy level and assess them in a psychophysical study to identify a perceptual scale of anisotropy. The generality of these scales is then verified by means of anisotropic surfaces appearance capturing using bidirectional texture function and its analysis on 3D objects. Eventually, we relate the perceptual scale of anisotropy to a computational feature obtained directly from anisotropic highlights observed in the captured reflectance data. The feature is validated using a psychophysical study analyzing visibility of anisotropic reflectance effects.

CCS Concepts

• ***Computing methodologies*** → ***Perception;*** *Reflectance modeling; Texturing;*

1. Introduction

Designers and manufacturers in many industries strive to create materials with unique light-transport properties, achieving an eye-catching look for their products. One approach to create an interesting appearance of an object is the introduction of a directional structure to its material. Directionality can be introduced, among other ways, by a combination of threads properties and weaving pattern in fabric, by wood fibers, or can be created by plastic molding or metal polishing. Directionality of material structure is related to material anisotropy. In general, anisotropy is the property of being directionally dependent, as opposed to isotropy, which implies identical properties in all directions. Anisotropic materials vastly expand the visual variability of isotropic appearance, due to the variable location of an anisotropic highlights [FK18]. Although anisotropic behavior is present to some extent in a majority of natural materials, its application to man-made surfaces is limited to materials like plastic and metal, where micro-structure can be easily introduced by surface finishing.

In this paper, we introduced managed appearance by utilizing 3D printing technology. We related the intensity of perceived directionality in material structure with perceived anisotropic reflectance effects caused, using a simple computational measure relying on data

DOI: 10.2312/pg.20191333

that can be conveniently captured. This tool can help designers to predict perceived intensity of anisotropic effects caused by certain types of material structures. Main contributions of the paper are following:

- We compare perceived anisotropy of (a) underlying texture pattern, (b) its planar 3D printed specimen, and (c) its rendering on shapes.
- We show a strong relationship between perceived macroscopic directionality and global anisotropic effect it causes.

2. Related Work

This paper builds upon research of the visual and computational assessment of anisotropy and its introduction in 3D printing.

Most of the work relating to anisotropy in computer vision deals with textural information. Past research studies psychophysical aspects of visual anisotropy [HHE08], [OVW11] and creates statistical models describing the relationship between perceived and computational textural anisotropy [Koe84], citeons11computational.Also in [FKH*18] was studied a relationship between physical and rendered material appearance. Norman [NTO04] shown that the extent of a highlight in any given direction is negatively related to the magnitude of curvature in that direction. Orientation structure of specular reflections appears to be a powerful source of information in visual perception [FTA04]. These studies have shown that people are good at recovering the 3D shape of perfectly mirrored objects. Distorted reflections across a specular surface provide a stable, powerful source of information about 3D shape. Giesel and Zaidi [GZ13] has shown that 3-D quality of material structure is a function of relative energy in corresponding 2-D frequency bands and relies on a relative contrast at particular spatial frequencies. The prediction of anisotropic highlights locations has already been studied [LKK00] and recently further extended to arbitrary geometry with interactive tangents editing [RGB*14]. A simplified method of anisotropic highlight detection for the purpose of adaptive measurement of anisotropic materials was shown in [FV15]. Filip [Fil15] used a database of BRDFs to analyze as to what extent people can detect anisotropy in renderings and proposed an approach to the anisotropic behavior detection in captured materials.

3D printing has been widely adopted for over a decade and utilized by various practitioners and professionals in industry. The most frequently used 3D printing process is a material extrusion technique called fused deposition modeling, creating a 3D object by adding material from melted filament, layer-by-layer based on CAD model geometry [TJ14].

We are not aware of any work combining 3D printing and visual psychophysics to creating and assessing controllable anisotropy of surface texture.

3. Proposed models of anisotropy

For analysis of visual perception of anisotropy one needs to employ an analytical model of anisotropic behavior allowing smooth transition from isotropic behavior to different levels of anisotropy. To introduce anisotropic behavior, we borrowed principles from real materials and composed our models of elliptical structural elements. The following two models were used:

3.1. Type A – stretching elements

We started with circular elements and modified them so as they become longer and narrower as the control parameter was increased. This behavior is typical for elastic fiber- or thread-based materials like fabric but the appearance of long fibers can be found also in wood texture, plastic molds, or metal finishing. Anisotropy is introduced by gradual stretching of the circles to elongated elliptic profiles. We start with semi-random distribution of circles in the texture, i.e., distribute their centers on a rectangular grid and randomly displaced them for half of a grid step. This helps to avoid the accumulation of elements in one spot and maintains spatial uniformity of the texture. The control parameter is length of the first ellipse's axis ($a = 1 \dots 6\ mm$), while the length of the second axis is reciprocal, i.e., $b = 1/a$. The first row of Fig. 2 illustrates the effect of the parameter.

3.2. Type B – changing orientation of elements

In this model we use fixed elongated elliptical shapes but randomly changed their orientation towards to more narrow distribution. This behavior is typical for elongated flakes in coatings that can uniform themselves either by rheology of an application process or by magnetic force [PLMR17]. We used ellipses (axes $a = 2.5\ mm, b = 0.4\ mm$) with their centers randomly distributed over the texture. As a control parameter was used an angle obtained in degrees as

$$\alpha = 180 \cdot (0.5 + (1 - \frac{i-1}{6}) \cdot [rand() - 0.5]) \ , \qquad (1)$$

where $rand()$ is a function generating a random number in range [0,1] and $i = 1 \dots 6$. This directional effect is illustrated in the second row of Fig. 2.

For the sake of continuous embossing when 3D printing, all elliptical elements are in fact elongated spheres, i.e., with the lowest intensity at their center. Alongside both anisotropic models, we also use as a reference anisotropic texture created by a sinusoidal pattern of vertical frequency comparable to the distribution of ellipses at the highest directionality level (see the most right column of Fig. 2).

4. From models to anisotropic material

Although, one could simulate appearance of the models directly by rendering their 3D texture and use it in psychophysical analysis, we decided to intermediate step of physical specimen fabrication using 3D printing before capturing its appearance. This approach has the benefit of visually assessing differences between perception of underlying texture, physical specimens, and their renderings.

4.1. Fabricating anisotropy

Once, we have texture models of anisotropy we use them to emboss 3D structures. We used OpenSCAD to create samples of size 65x65mm with a height variation around 1mm. The size of initial elements was adjusted to 2-5mm so as they can be safely reproduced and not affected by the spatial accuracy of the printing. The 3D printer used was an Original Prusa i3 MK2 with layer height 0.05mm and 0.4mm nozzle. We used 1.75mm white filaments to force subjects to assess only macroscopic directionality and not the

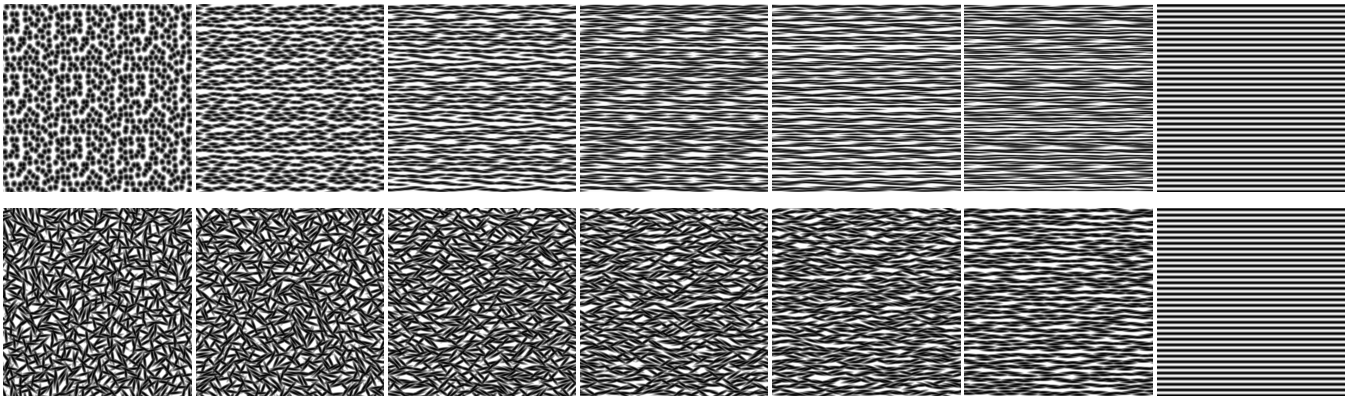

Figure 2: *Textures used as height profile of 3D printed surfaces: anisotropy of type A and B, respectively.*

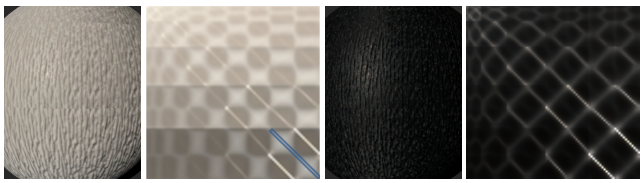

Figure 3: *An example of anisotropy of Type A captured as BTF (odd images) and its BRDF (even images) for white and black filaments. The highlighted area in left material shows a data slice used for the proposed computational prediction of anisotropy.*

anisotropic highlights it causes. Printing time of one planar sample was around one hour. The prints for both types of anisotropy are shown in Fig. 1.

4.2. Rendering fabricated anisotropy

Eventually, to obtain a realistic visualization of printed material appearance, we captured the 3D printed planar patches as bidirectional texture functions [DvGNK99]. We used angular sampling as proposed in [SSK03] providing hemispherically uniform sampling of 81 viewing and 81 illumination directions, which is convenient for our diffuse printed samples. Altogether we performed 13 measurements each comprising of 6,561 images. This data allows us to visualize the captured appearance on any 3D object. For the sake of our psychophysical studies, we used sphere and car-like objects. Examples of visualized captured appearance are shown in first and third images of Fig. 3.

5. Perception of controlled anisotropy

This section describes a psychophysical evaluation of the same anisotropy in textures (experiment 1), their fabricated specimens (experiment 2), and their captured appearance (experiment 3).

5.1. Methodology

Experiments 1 and 3 with textures and renderings were done online in uncontrolled conditions, while Experiment 2 was done in person under controlled conditions. In all experiments, subjects were asked to assess level of anisotropy of the tested sample (texture/specimen/rendering). To help the subject establish personal scales of anisotropy, we accompanied each stimuli (in the middle) with reference isotropic sample (left) and extremely anisotropic sample (right). To provide sufficient options for the subjects, we used an eleven-point Likert-like rating scale, where 0 corresponds to the lowest and 10 to the highest level of anisotropy. To get insight into typical subjects' responses we computed the mean opinion score obtained as average rating across all subjects.

***Experiment 1**: Anisotropy in texture* – In this online experiment we collected responses from 80 anonymous subjects. Subjects performed the study with 12 stimuli (2 types $\times$ 6 levels) on average in 83 seconds.

***Experiment 2**: Anisotropy in 3D prints* – eleven paid subjects performed the experiment in one session. Their ages ranged from 23 to 44, four were male and seven female. All subjects had normal or corrected to normal vision, and all were uninformed with respect to the purpose and design of the experiment. As subjects should observe the samples synchronously, we created a simple rotation table with three synchronized rotating platforms each holding one specimen as shown in Fig.4 (left: isotropic, middle: the sample in query, right: extreme anisotropy). Subjects were free to rotate the samples as long as they want. The table was illuminated by a desk light. Evaluation of 10 samples (2 types $\times$ 5 levels, i.e. isotropic variant not tested) took on average around 15 minutes, most of which was sample manipulation time.

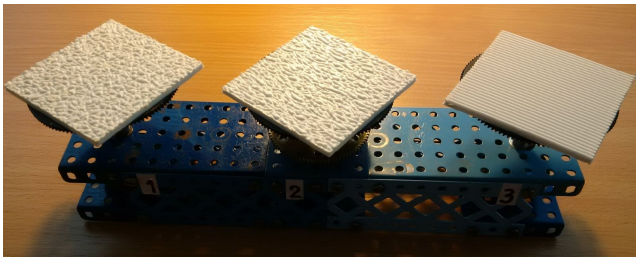

Figure 4: *A setup for simultaneous comparison of three printed specimens in Experiment 2.*

***Experiment 3**: Directionality in captured appearance* – In this online experiment we collected responses from 82 anonymous subjects. We tested both anisotropy types on two objects (with different

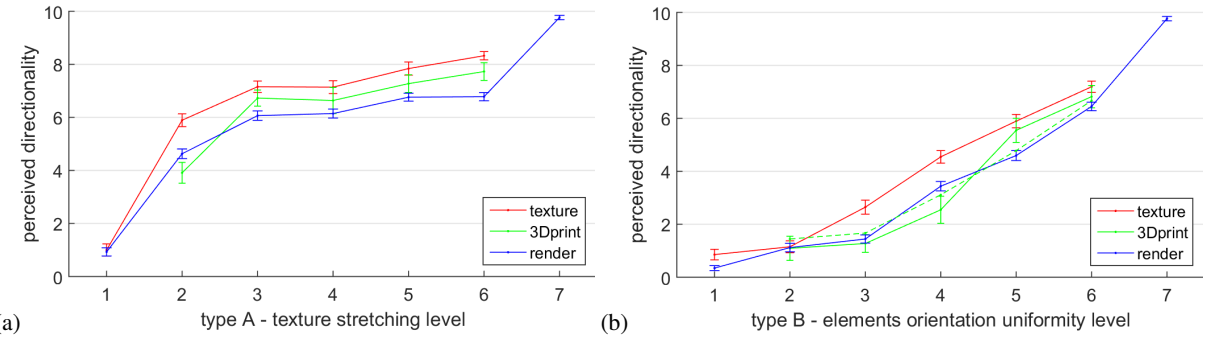

Figure 5: *Perceived anisotropy in texture (red), physical specimen (green), and renderings of captured appearance (blue): (a) type A – elements stretch, (b) type B – elements orientation.*

texture scales), while for the second object we tested two different anisotropy axis alignments. As we included also reference images and two images for different filament materials, we obtained 42 stimuli (2 anisotropy types × (car 2 axis rotation + sphere) × 7). On average subjects finished the experiment in 270 seconds.

5.2. Results

This section summarizes results of all three experiments. In each experiment we computed mean opinion scores across all subjects, consistency of subjects' responses was assessed using standard error visualized as errorbars.

Types of anisotropy – first we compared perception of two tested types of anisotropy in all three experiments. Results are shown in Fig. 5. For each type we observe different sensitivity to surface directionality as a function of anisotropy control parameter. For Type A (elements stretch) subjects were more sensitive to an initial stretch, while stretching beyond a>3 was considered visually very similar. On the contrary, the increase of perceived anisotropy of Type B (elements uniformity) was almost linear. For both anisotropy types we observe very similar subject responses for all three experiments. In general values for the experiment with textures (red outline) are slightly higher than for experiments with specimens and renderings, which might be due to high contrast in the texture and thus better visibility of structures. Although the number of subjects, especially for the experiment with specimens, was limited, we note high consistency among the subjects as demonstrated by low standard errors. We also tested reliability of the subjects' data from all experiment using Krippensdorf alpha and obtained relatively high values between 0.52 and 0.71. Hypotheses testing of individual anisotropy levels means using repeated measures ANOVA, and Friedman tests confirmed significant differences with p-values below 0.00002.

6. Predicting anisotropic effects from appearance data

In the previous section, we assessed perception of directionality on a macroscopic scale. However, this structure influences global material appearance by the introduction of global anisotropic highlights. In this section, we look for relationship between perceived anisotropy as marcoscopic directionality in printed structures, and global directional anisotropic appearance. We suggest a computational measure predicting perceived anisotropy purely from directional textureless data.

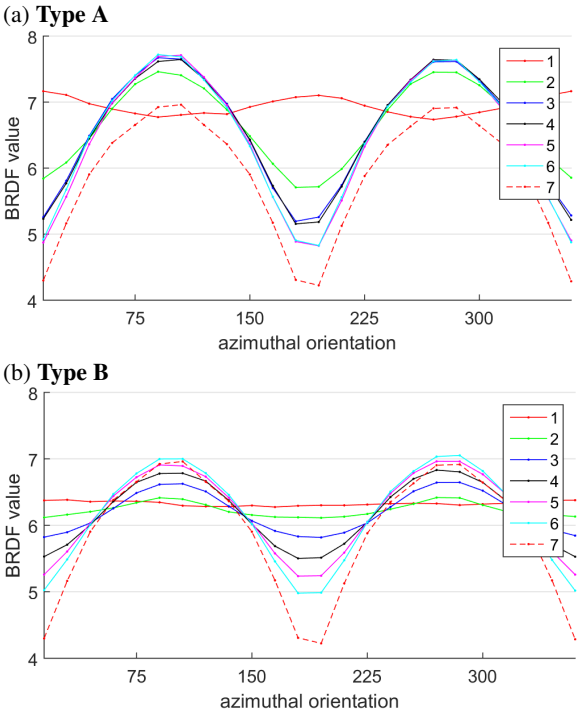

Figure 6: *Azimuthally dependent analysis of BRDF slices at view and light elevation angles 75° for individual levels of (a) Type A and (b) Type B anisotropy.*

When moving away from the material to a distance when the structure becomes indistinguishable one could observe only the highlights, without the texture. At such distance, individual textures in BTF can be safely substituted by their representative values stored as a BRDF [FVHK17], i.e., only RGB values holding information on angular-dependent reflectance behavior including anisotropy. Fig. 3 shows BRDF printed anisotropy of Type A in a form of 2D images, where we can observe clear anisotropic behavior in 81 viewing (horizontal axis) and illumination (vertical axis) directions demonstrated by variable intensity along image diagonal direction. We have computed BRDF for both anisotropy types at all tested control levels (see supplementary material), where one can observe a gradual increase of anisotropy levels as a function of

the control level. For our analysis we use radiometrically calibrated BRDF data to CIE Luminance for illuminant D65.

As anisotropic behavior is most distinct for grazing angles [Fil15], we selected elevations $\theta_i = 75^\circ, \theta_v = 75^\circ$ and small difference between illumination and viewing azimuths. We fixed mutual positions of light and camera azimuths to $\|\varphi_i - \varphi_v\| = 15^\circ$ and for 24 azimuths recorded a slice B in BRDF angular space. See the second image in Fig. 3, for the location of the slice. The slice can be conveniently captured by rotating the sample for under fixed illumination and viewing conditions. Such slices for individual control levels of both anisotropy types are shown in Fig. 6. Here, one can observe changes of slice reflectance as a function of the control parameter from almost constant isotropic behavior to different levels of anisotropy. The first graph reveals that even the initial structure of semi-randomly positioned circles (solid red outline) has already some anisotropic behavior.

We tested several features to proportionally approximate perceived directionality in 3D prints from slice's reflectance values. We converged to the one based on a combination of perceived directionality approximated as maximum value of absolute difference between anisotropic slice B and mean value of isotropic slice $\bar{B}_{iso}$, and its absolute scaling according to the Weber's law [FBH66]. Additionally, we have to account not only for a difference between absolute values in the slice, but also for a contrast of intensity values near the anisotropic highlight. This contrast is related to a width of the highlight. Therefore, we normalize the maximal value of anisotropic highlight by its neighbouring value B_N captured 15° apart from azimuthal positions of light and camera

$$A_C = \max\left(\frac{\|B/B_N - \bar{B}_{iso}\|}{\bar{B}_{iso}}\right) . \qquad (2)$$

This increases response for narrow highlights, without need of additional measurements. The angular difference 15° should be sufficient as anisotropic effects introduced by 3D printing do not typically produce more narrow highlights.

This measure is also quite intuitive as it evaluates absolute difference of intensities between isotropic value and the strongest visible anisotropy effect. This measure (2) has also high correlations with perceived anisotropy obtained in the experiment 3 on rendered data. The Pearson correlation for Type A was 0.986 (p-value $4.3 \cdot 10^{-5}$), and for Type B was 0.977 (p-value $1.5 \cdot 10^{-4}$). Fig. 7 depicts results of the measure (solid outlines) overlaid by results of the Experiment 3 (dashed outlines) scaled by linear fitting. The main difference is in the first level of Type A anisotropy, which is in fact isotropic surface, where computational measures detect some level of anisotropy, is due to the fact that in psychophysical experiments this surface is enforced as isotropic as it was used as isotropic reference. This might be a reason for the higher value of the measure.

7. Perceived directionality vs. anisotropic effects

In the previous sections we psychophysically analyzed perceived directionality in printed surfaces and proposed a computational measure for its prediction. In this section, we psychophysically analyze solely the anisotropic reflectance effects caused by a directional structure. One can imagine moving further from the object with the printed anisotropic structure so as one cannot see details,

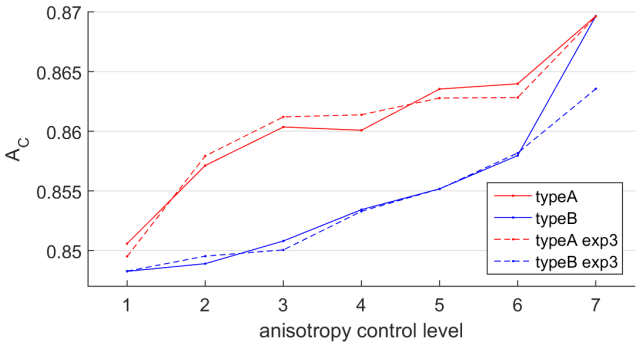

Figure 7: *Anisotropy prediction computed from BRDF slice at elevations 75° (solid outlines), compared to perceived directionality in rendered images (dashed outlines).*

but only anisotropic highlights. To achieve this, we use rendering of captured BRDF reflectance obtained by averaging of BTF images.

For this analysis we printed a new set of samples. As we prefer better visibility of anisotropic effects, we used black filament. We printed again six levels of Type B anisotropy and the reference sinusoidal grating. Although the color and scale of structure was different we obtained in Experiment 2 nearly identical results to those using white filament (compare the full and dashed green lines in Fig. 5-b).

***Experiment 4**: Anisotropy in captured reflectance* – Once we obtained BRDFs of printed samples, we use them for preparation of stimuli images for the psychophysical experiment. We used a scene with spheres, having simple geometry with predictable location of anisotropic highlights. We use the same principle as in previous experiments, i.e., relating visual appearance of image in the middle on a scale 0-10 to the reference images of minimum/maximum anisotropic effect on the left/right (see example of stimulus image in Fig. 8). A total of 55 subjects participated in our online study. After computing mean opinion scores, we obtained the results shown as the green outline in Fig. 9. This figure includes also results of perceived structure from physical specimens in Experiment 2 and predicted response of the proposed measure (2). Note, that we performed a linear fitting of the data from the experiments, to obtain approximately the same scaling as the measure. Obviously the scaling constants (shown in figure as K) were different, as perceived directionality responses to printed surfaces were generally higher than responses to anisotropic reflectance patterns. However, the scaled version show a good alignment with the proposed anisotropic measure demonstrating clear relation between perceived directionality and its causal anisotropic effects.

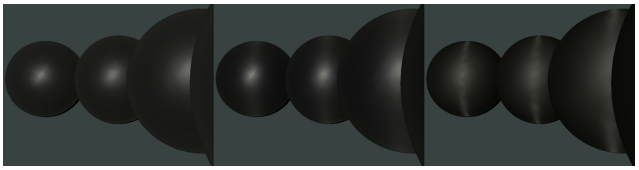

Figure 8: *An example of Experiment 4 stimuli image.*

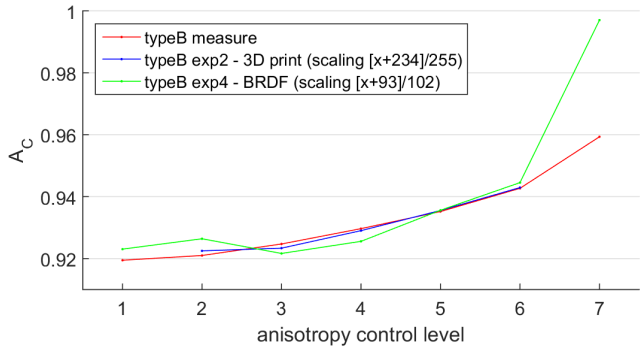

Figure 9: *A comparison of the proposed measure (red outline) with scaled responses of perceived physical directionality (blue outline) and its perceived reflectance effects (green outline). Material: black filament.*

8. Discussion and Future work

Our analysis has several limitations. We have tested only a white diffuse and black materials. The diffuse white material was used intentionally so as subjects are assessing only the macroscopic directionality and are not influenced by the consequentially created global anisotropic highlights. In contrast, the black material was used to suppress visibility of directional structures, but enhance visibility of related anisotropic effect. It would be interesting to verify our conclusions on different 3D printable materials. We also focused only on two types of anisotropic behavior. Although they should cover many real-world sources of anisotropy, material appearance can get more complicated when multi-modal anisotropy occurs, which is quite common, e.g., in fabric materials.

We assume that the proposed anisotropic measure is a promising candidate for predicting both perceived directionality and anisotropy level. Due to its convenient capturing, it can be easily used by practitioners to assess extent of perceived anisotropic effects. We show responses of the proposed measure on radiometrically calibrated CIE luminance data of two extreme materials (diffuse white and shiny black), so one can relate any additional measurement to the absolute scales provided. In future work, we plan to find absolute scaling between perceived directionality and related perceived anisotropic effect introduced, that can be generalized also on different classes of anisotropic materials.

9. Conclusions

We have shown, that 3D printing techniques can be used to fabricate materials with variable anisotropic properties. We created two sets of anisotropic samples with a controlled directionality level in a 3D printed macro-structure. This work, identified the relationship between perceived macroscopic directionality, perceived anisotropic effects. We used visual psychophysics to compare these macroscopic directional effects with the global anisotropic effect it created. The perception of directionality was stable regardless of real vs. rendered stimuli, texture scale, surface shape, and orientation. Finally, we suggest a computational measure of anisotropy derived from the created anisotropic effect captured in a BRDF slice, which is proportional to the perceived directionality data.

Acknowledgments

We would like to thank Petr Vaníček from ÚTIA for 3D printing of samples, and all volunteers taking part in the psychophysical experiment. This research has been supported by the Czech Science Foundation grant 17-18407S.

References

[DvGNK99] DANA K., VAN GINNEKEN B., NAYAR S., KOENDERINK J.: Reflectance and texture of real-world surfaces. *ACM Trans. on Graphics 18*, 1 (1999), 1–34. 3

[FBH66] FECHNER G., BORING E., HOWES D.: *Elements of psychophysics*. The Morgan Kaufmann Series in Computer Graphics. New York, Holt, Rinehart and Winston, 1966. 5

[Fil15] FILIP J.: Analyzing and predicting anisotropic effects of BRDFs. In *ACM SAP* (2015), pp. 25–32. 2, 5

[FK18] FILIP J., KOLAFOVÁ M.: Perception of Car Shape Orientation and Anisotropy Alignment. In *Workshop on Material Appearance Modeling* (2018), Klein R., Rushmeier H., (Eds.), The Eurographics Association. 1

[FKH*18] FILIP J., KOLAFOVÁ M., HAVLÍČEK M., VÁVRA R., HAINDL M., RUSHMEIER H.: Evaluating Physical and Rendered Material Appearance. *The Visual Computer (Computer Graphics International 2018)*, 6-8 (2018), 805–816. 2

[FTA04] FLEMING R. W., TORRALBA A., ADELSON E. H.: Specular reflections and the perception of shape. *Journal of Vision 4*, 9 (2004), 10. 2

[FV15] FILIP J., VAVRA R.: Anisotropic materials appearance analysis using ellipsoidal mirror. In *IS&T/SPIE Conference on Measuring, Modeling, and Reproducing Material Appearance, paper 9398-25* (2015). 2

[FVHK17] FILIP J., VÁVRA R., HAVLÍCEK M., KRUPICKA M.: Predicting visual perception of material structure in virtual environments. *Computer Graphics Forum 36*, 1 (2017), 89–100. 4

[GZ13] GIESEL M., ZAIDI Q.: Frequency-based heuristics for material perception. *Journal of vision 13*, 14 (2013), 7. 2

[HHE08] HANSEN B. C., HAUN A. M., ESSOCK E. A.: The horizontal effect: A perceptual anisotropy in visual processing of naturalistic broadband stimuli. In *Visual Cortex: New Research*. 2008. 2

[Koe84] KOENDERINK J. J.: The structure of images. *Biological cybernetics 50*, 5 (1984), 363–370. 2

[LKK00] LU R., KOENDERINK J. J., KAPPERS A. M.: Specularities on surfaces with tangential hairs or grooves. *Computer Vision and Image Understanding 78*, 3 (2000), 320–335. 2

[NTO04] NORMAN J. F., TODD J. T., ORBAN G. A.: Perception of three-dimensional shape from specular highlights, deformations of shading, and other types of visual information. *Psychological Science 15*, 8 (2004), 565–570. 2

[OVW11] ONS B., VERSTRAELEN L., WAGEMANS J.: A computational model of visual anisotropy. *PLoS ONE 6*, 6 (2011), e21091. 2

[PLMR17] PEREIRA T., LEME C. L. A. P., MARSCHNER S., RUSINKIEWICZ S.: Printing anisotropic appearance with magnetic flakes. *ACM Trans. Graph. 36*, 4 (July 2017), 123:1–123:10. 2

[RGB*14] RAYMOND B., GUENNEBAUD G., BARLA P., PACANOWSKI R., GRANIER X.: Optimizing BRDF orientations for the manipulation of anisotropic highlights. In *Computer Graphics Forum* (2014), vol. 33, Wiley Online Library, pp. 313–321. 2

[SSK03] SATTLER M., SARLETTE R., KLEIN R.: Efficient and realistic visualization of cloth. In *Eurographics Symposium on Rendering* (2003), pp. 167–178. 3

[TJ14] TAUFIK M., JAIN P.: Role of build orientation in layered manufacturing: A review. *International Journal of Manufacturing Technology and Management 27* (01 2014), pp.47 – 73. 2